

## Changes in Cerebral Hemodynamics and Progression of Subclinical Vascular Brain Disease

### A Population-Based Cohort Study

Ma, Yuan; Bos, Daniel; Wolters, Frank J.; Niessen, Wiro; Hofman, Albert; Ikram, M. Arfan; Vernooij, Meike W.

**DOI**

[10.1161/STROKEAHA.124.047593](https://doi.org/10.1161/STROKEAHA.124.047593)

**Publication date**

2024

**Document Version**

Final published version

**Published in**

Stroke

**Citation (APA)**

Ma, Y., Bos, D., Wolters, F. J., Niessen, W., Hofman, A., Ikram, M. A., & Vernooij, M. W. (2024). Changes in Cerebral Hemodynamics and Progression of Subclinical Vascular Brain Disease: A Population-Based Cohort Study. *Stroke*, *56* (2025)(1), 95-104. Article 047593. <https://doi.org/10.1161/STROKEAHA.124.047593>

**Important note**

To cite this publication, please use the final published version (if applicable). Please check the document version above.

**Copyright**

Other than for strictly personal use, it is not permitted to download, forward or distribute the text or part of it, without the consent of the author(s) and/or copyright holder(s), unless the work is under an open content license such as Creative Commons.

**Takedown policy**

Please contact us and provide details if you believe this document breaches copyrights. We will remove access to the work immediately and investigate your claim.

***Green Open Access added to TU Delft Institutional Repository***

***'You share, we take care!' - Taverne project***

**<https://www.openaccess.nl/en/you-share-we-take-care>**

Otherwise as indicated in the copyright section: the publisher is the copyright holder of this work and the author uses the Dutch legislation to make this work public.

## ORIGINAL CONTRIBUTION

# Changes in Cerebral Hemodynamics and Progression of Subclinical Vascular Brain Disease: A Population-Based Cohort Study

Yuan Ma<sup>1</sup>, MBBS, PhD; Daniel Bos<sup>2</sup>, MD, PhD; Frank J. Wolters<sup>2</sup>, MD, PhD; Wiro Niessen, PhD; Albert Hofman<sup>2</sup>, MD, PhD; M. Arfan Ikram<sup>2</sup>, MD, PhD; Meike W. Vernooij<sup>2</sup>, MD, PhD

**BACKGROUND:** Cerebral hypoperfusion is associated with vascular brain injury and neurodegeneration, but their longitudinal relationship is largely unknown, especially in healthy older adults.

**METHODS:** We investigated the longitudinal relationship between cerebral hemodynamics and subclinical vascular brain disease in community-dwelling older adults without stroke or dementia at baseline. Participants underwent brain magnetic resonance imaging scans every 3 to 4 years between 2005 and 2016. Cerebral blood flow (CBF) was measured through 2-dimensional phase-contrast magnetic resonance imaging; the cerebrovascular resistance index (CVRI) was defined as the ratio of mean arterial blood pressure to total CBF. Simultaneous progression in subclinical brain disease was evaluated through repeated magnetic resonance imaging assessment of white matter hyperintensities (WMH), cerebral microbleeds, lacune, and brain atrophy. The longitudinal relationship was estimated using generalized estimating equations, with adjustment for age, sex, smoking habits, body mass index, systolic blood pressure (for CBF measures), lipid level, history of diabetes and cardiovascular disease, and the baseline burden of magnetic resonance imaging markers.

**RESULTS:** Among 3623 older adults (mean age, 61.4±9.3 years; 54.6% women), large decreases and increases in CBF and increases in CVRI over time were associated with white matter hyperintensity progression. The risk ratios for white matter hyperintensity progression were 1.36 (95% CI, 1.19–1.55) for large decreases in total CBF (lowest quartile), 1.02 (95% CI, 0.91–1.14) for moderate decreases (second quartile), and 1.28 (95% CI, 1.14–1.45) for large increases (highest quartile), compared with stable CBF (third quartile). The corresponding risk ratios for changes in CVRI were 1.13 (95% CI, 1.00–1.30), 1.25 (95% CI, 1.09–1.43), and 1.33 (95% CI, 1.16–1.52) for the second to fourth (versus lowest) quartiles, respectively, showing a dose-response relationship. The changes in CBF also demonstrate a similar U-shaped association with the progression of brain atrophy and incident microbleeds, whereas increases in CVRI were associated with lower microbleed risk.

**CONCLUSIONS:** Longitudinal changes in CBF and CVRI may capture distinct pathophysiologies linking cerebral hemodynamics to subclinical brain disease, extending beyond single-time point measurements.

**GRAPHIC ABSTRACT:** A graphic abstract is available for this article.

**Key Words:** blood pressure ■ brain injuries ■ cerebral small vessel diseases ■ cerebrovascular circulation ■ magnetic resonance imaging

Despite accounting for only 2% of the body weight, the brain receives about 20% of the total arterial blood supply, making it highly perfused and susceptible

to cerebral hypoperfusion.<sup>1</sup> Prolonged hypertension and aging can compromise cerebral autoregulation mechanisms responsible for maintaining stable cerebral blood

Correspondence to: Yuan Ma, MBBS, PhD, Department of Epidemiology, Harvard T.H. Chan School of Public Health, 677 Huntington Ave, Boston, MA 02115, Email [yuanma@hsph.harvard.edu](mailto:yuanma@hsph.harvard.edu); or Meike W. Vernooij, MD, PhD, Department of Radiology and Nuclear Medicine, Erasmus MC University Medical Center, PO Box 2040, 3000 CA Rotterdam, the Netherlands, Email [m.vernooij@erasmusmc.nl](mailto:m.vernooij@erasmusmc.nl)

Supplemental Material is available at <https://www.ahajournals.org/doi/suppl/10.1161/STROKEAHA.124.047593>.

For Sources of Funding and Disclosures, see page XXX.

© 2024 American Heart Association, Inc.

Stroke is available at [www.ahajournals.org/journal/str](http://www.ahajournals.org/journal/str)

## Nonstandard Abbreviations and Acronyms

<b>BP</b>	blood pressure
<b>CBF</b>	cerebral blood flow
<b>MRI</b>	magnetic resonance imaging
<b>pCBF</b>	parenchymal cerebral blood flow
<b>tCBF</b>	total cerebral blood flow
<b>WMH</b>	white matter hyperintensities

flow (CBF),<sup>2–4</sup> potentially exposing the brain to cerebral hypoperfusion, hypoxia, ischemia, and consequently, stroke and dementia.<sup>5,6</sup> Despite epidemiological studies linking cerebral hypoperfusion to dementia and stroke, the interrelationship and underlying mechanisms during the subclinical phase remain unclear.<sup>7–10</sup> This knowledge gap is partly because of the limitations of single-time point measurements of CBF, which are insufficient to capture the pathophysiology of cerebral hemodynamics and overlook the interaction between CBF and arterial pressure that affects downstream vascular resistance.

Studies linking lower CBF to subclinical brain disease including brain atrophy and cerebral small vessel disease are largely limited by small sample sizes and inconsistent results.<sup>11–15</sup> Single-time point measurements of CBF vary substantially between individuals.<sup>16,17</sup> Monitoring changes in CBF over time within the same individuals may provide valuable insights into its dynamic nature and enable the detection of subtle progression in cerebral hemodynamic disturbances. Indeed, CBF is generally observed to decline with aging and hypertension,<sup>18–20</sup> but there is limited data on the relationship between longitudinal changes in CBF and the progression of subclinical brain vascular disease, especially in the unselected general older population. Understanding this relationship is crucial for elucidating the cause of stroke and dementia at the early subclinical stages, thus providing more opportunities for early interventions. Moreover, emerging data suggest that cerebrovascular resistance of cerebral arteries and arterioles, a fundamental mechanism for maintaining stable CBF in response to changes in blood pressure (BP),<sup>21</sup> is more sensitive than CBF for detecting early brain pathologies and cognitive impairment.<sup>22,23</sup> However, its relationship with subclinical brain disease in community-dwelling older adults remains to be determined. In the current study, we investigated the association of longitudinal changes in cerebral hemodynamics, operationalized as changes in CBF and cerebrovascular reactivity index, with the progression of subclinical brain disease, leveraging repeated brain magnetic resonance imaging (MRI) measurements in the Rotterdam Study. We hypothesized that changes in CBF and cerebrovascular reactivity index over time would better capture impaired cerebral hemodynamics and their association with vascular brain injury than single-time point measurements.

## METHODS

Data cannot be made available in a public repository owing to legal and ethical restraints but can be made available to interested researchers on request to the data manager Frank J.A. van Rooij (f.vanrooij@erasmusmc.nl). The analytical code is available from the corresponding author on reasonable request.

### Study Design and Participant Selection

The study is embedded in the Rotterdam Study, an ongoing prospective cohort study initiated in 1990 in Rotterdam, the Netherlands.<sup>24</sup> Briefly, 7983 participants aged  $\geq 55$  years were recruited in 1990, with 3011 participants aged  $\geq 55$  years added in 2000 and 3932 participants aged  $\geq 45$  years further added in 2005. Follow-up visits are performed approximately every 3 to 4 years. Brain MRI has been implemented in the core protocol of the Rotterdam Study since 2005, and participants without MRI contraindications were invited to repeat MRI scans during follow-up visits every 3 to 4 years.<sup>25</sup> As of September 2015, 6216 participants (91% of 6799 eligible invitees) underwent an MRI exam, out of which, 5680 participants completed all the MRI sequences and provided usable imaging data. The present study includes all participants who completed at least 2 MRI scans ( $n=3744$ ). After further excluding participants developing dementia or stroke before follow-up MRI ( $n=121$ ), 3623 participants were eligible for the current study, contributing to a total of 9282 eligible MRI scans with a median scan interval of 3.6 years. In addition, for the analyses involving brain volumetric measures and CBF measures, 97 (2.8%) participants with supratentorial cortical infarcts or suboptimal MRI segmentation were excluded (Figure S1). Participants with  $\geq 2$  eligible MRI scans were younger and had healthier vascular profiles compared with participants with only one eligible MRI scan (Table S1).

The Rotterdam Study has been approved by the Medical Ethics Committee of the Erasmus MC and by the Dutch Ministry of Health, Welfare, and Sport. The Rotterdam Study has been entered into the Netherlands National Trial Register (<https://onderzoekmetmensen.nl>) and the World Health Organization International Clinical Trials Registry Platform under shared catalog number NTR6831. All participants provided written informed consent to participate in the study and to have their information obtained from treating physicians. The current study is reported according to the Strengthening the Reporting of Observational Studies in Epidemiology guideline.

### Brain MRI Scan

Brain MRI was performed at each time point on a single 1.5T MRI scanner (GE Healthcare) using a standardized protocol.<sup>25</sup> Four high-resolution axial sequences were obtained, including a T1-weighted sequence, a proton density-weighted sequence, a fluid-attenuated inversion recovery sequence, and a T2\*-weighted gradient recalled echo sequence. No contrast material was administered. CBF was quantified using 2-dimensional phase-contrast imaging as described previously.<sup>26</sup> In short, blood flow velocity (mm/s) was measured using manually drawn regions of interest on the 2-dimensional phase-contrast images in both carotids and the basilar artery at a level just under the skull base. Flow rates were calculated from the velocity and cross-sectional area of the vessels. Orthogonality

of the carotid and basilar arteries was ensured by applying the sagittal 2-dimensional phase-contrast MRI angiographic scout image to localize the phase-contrast imaging plane perpendicular to the carotid and basilar arteries.<sup>26</sup>

### Cerebral Hemodynamic Measures

We first assessed CBF and its change over 2 sequential scans an average of 3.6 years apart. CBF was quantified as total CBF (tCBF in mL/min) or parenchymal CBF (pCBF in mL·100 mL<sup>-1</sup>·min<sup>-1</sup>). tCBF was determined by adding flow rates for the carotid arteries and the basilar artery and expressed in mL/min. Two independent, experienced technicians drew all the manual regions of interest and performed subsequent flow measurements. Double rating performed in 533 scans yielded high inter-rater correlations of >0.94 for all vessels, suggesting excellent agreement. pCBF (mL·min<sup>-1</sup>·100 mL<sup>-1</sup>), which reflects the flow within a defined volume of tissue, was derived by dividing tCBF (mL/min) by total brain tissue volume measured at the same time (per 100 mL, defined as the sum of the volume of gray matter and white matter). Changes in CBF were defined as the change in tCBF (or pCBF) over 2 sequential visits divided by scan intervals. As longitudinal changes in pCBF are determined by changes in tCBF and brain tissue volume, which can complicate the interpretation, we primarily assessed the change in tCBF while adjusting for total brain tissue volume as a covariate, but we also repeated the analyses for changes in pCBF. We furthermore assessed the cerebrovascular resistance index and its change across sequential scan intervals. Cerebrovascular resistance index was defined as the ratio of cerebral perfusion pressure (=mean arterial BP–intracranial pressure) to tCBF. Given intracranial pressure is much lower than mean arterial BP, the cerebrovascular resistance index is estimated as the ratio of mean arterial BP to tCBF.<sup>21</sup> Mean arterial BP was derived as one-third of systolic BP and two-thirds of diastolic BP.

### Brain Structural Measures

Supratentorial brain tissue volumes, including gray matter, white matter, and white matter hyperintensities (WMH), were quantified using automated brain tissue segmentation and were inspected visually and corrected manually if needed.<sup>25,27</sup> Total brain tissue volume was defined as the sum of the volume of gray matter, normal-appearing white matter, and WMH. To correct for head size, all these volumetric measures were expressed as the percentage of total intracranial volume (ie, the sum of gray and white matter and cerebrospinal fluid volumes). Focal markers of cerebral small vessel disease were visually rated by trained research physicians.<sup>25</sup> Specifically, lacunes were defined as subcortical lesions ≥3 mm and <15 mm with the same signal intensity as cerebrospinal fluid on all sequences and a hyperintense rim on fluid-attenuated inversion recovery sequence in the supratentorial region. Microbleeds were defined as focal round to ovoid areas <10 mm of low signal intensity on 3-dimensional high-resolution T2\*-weighted gradient recalled echo sequence.

The progression of subclinical brain vascular disease over a rolling time window of 2 sequential scans was assessed using methods similar to those described above for CBF.<sup>28</sup> Specifically, the progression of lacunes was defined as having ≥1 new lacunes on the second scan. The progression of microbleeds was defined as having ≥1 new microbleed on the second scan. The progression of WMH was defined as the rate of increase in WMH volume (ie, volume changes divided by the scan intervals)

within the highest quartile. Similarly, the progression of brain atrophy was defined as the highest quartile of the decline rate in total brain tissue volume. The progression of WMH volume and brain atrophy were dichotomized for comparable interpretations with the focal MRI markers of microbleeds and lacunes.

### Assessment of Other Variables

Information on demographic characteristics was collected at the first visit. During each visit, smoking habits, body mass index, and medication use were assessed with standardized protocols. Two BP measurements were taken on the right upper arm at each visit after at least 5 minutes of rest in a seated position. Hypertension was defined as a resting BP exceeding 140/90 mm Hg or the use of BP-lowering medication. Diabetes was defined as a fasting glucose level of ≥7.0 mmol/L or the use of antidiabetic medication. Cardiovascular diseases, including coronary heart disease, heart failure, and atrial fibrillation, were assessed via interviews and verified by medical records.<sup>24,29</sup>

### Statistical Analysis

We assessed the bidirectional relationship between cerebral hemodynamic measures and subclinical brain vascular disease in 3 steps: the relationships between (1) a single measurement of cerebral hemodynamics and the progression of subclinical brain vascular disease during the subsequent scan intervals, (2) the presence of subclinical brain vascular disease at baseline and changes in cerebral hemodynamics during the subsequent scan interval, and (3) simultaneous changes in cerebral hemodynamics and subclinical brain vascular disease during the same scan interval, with details described below.

### Cerebral Hemodynamics at Baseline and Subsequent Progression of Subclinical Brain Vascular Disease

We assessed the association of a single measurement of cerebral hemodynamics at baseline (defined as the first of 2 consecutive scans) with the progression of individual markers of subclinical brain vascular disease (including WMH, lacunes, microbleeds, and brain atrophy as binary outcomes) during the subsequent scan intervals. Generalized estimating equations with empirically calculated SEs were used to account for the correlation of repeated observations within the same participant.<sup>30</sup> Poisson regression was used to model the incidence rate of progression for subclinical vascular disease markers over different time intervals and to estimate the incidence rate ratio; if lesions regressed, they were entered as zero counts (ie, absence of progression). Both continuous and quartile-based categorical variables of cerebral hemodynamic measures were assessed as the primary exposures. Test for nonlinear trend was conducted using restricted cubic splines.<sup>31</sup> To control for possible confounding factors, we adjusted for age, sex, smoking habits, body mass index, systolic BP (for tCBF and pCBF as the exposures), total cholesterol level, history of diabetes and cardiovascular disease, the baseline level of the individual MRI marker, and total brain tissue volume (for tCBF and cerebrovascular resistance index as the exposures) in the final models. We adjusted for baseline brain MRI markers because it has been indicated that adjusting for baseline outcome variables can correctly control regression-to-the-mean effect in nonrandomized studies in which baseline outcome influences the exposure.<sup>32</sup>

### Subclinical Brain Vascular Disease at Baseline and Subsequent Changes in Cerebral Hemodynamics

Second, we assessed the association of subclinical brain vascular disease at baseline with the rate of change in cerebral hemodynamic measures during the subsequent scan using linear regression in generalized estimating equation models as described above. We built the model for each MRI biomarker of the subclinical brain vascular disease (including WMH volume, lacunes, microbleeds, and total brain tissue volume) separately. We adjusted for age, sex, body mass index, systolic BP, total cholesterol level, smoking habits, history of diabetes and coronary heart disease, cerebral hemodynamic measurement, and total brain tissue volume at the time of the initial MRI scan.

### Simultaneous Changes in Cerebral Hemodynamics and Subclinical Brain Vascular Disease

We assessed the association of changes in cerebral hemodynamic measures with the progression of individual markers of subclinical brain vascular disease during the same scan using the same methods as described above for the association between a single measurement of cerebral hemodynamic measures with subsequent progression of subclinical brain vascular disease, with additional adjustment for baseline cerebral hemodynamic measures.

### Other Secondary and Sensitivity Analyses

To further account for the potential confounding role of BP and antihypertensive medication use, we replaced systolic BP with diastolic BP and antihypertensive medication use in separate models and performed the analyses stratified by hypertension status. We additionally adjusted for longitudinal changes in systolic BP in separate models, given that it could confound or potentially mediate the association of interest. Given the interrelationship between CBF and hemoglobin in maintaining cerebral oxygen supply and their association with dementia reported in a previous study,<sup>33</sup> we further adjusted for hemoglobin level. In addition, to account for the potential selection bias of including participants with repeated brain MRI assessment in the analyses, we further assessed the association employing inverse probability weights constructed using baseline covariates. Finally, we assessed microbleeds in the lobar region (indicative of cerebral amyloid angiopathy) and deep region (indicative of hypertension-related pathology), respectively. Missing data (ranging from 0% to 9.3% for the covariates) were handled using a missing indicator approach. Statistical analyses were performed using SAS version 9.4 (SAS Institute, Inc).

## RESULTS

Of 3623 participants, 1978 (54.6%) were women and the mean (SD) age at the first MRI scan was 61.4 (9.3) years. Table 1 describes the participant characteristics and cerebral hemodynamic measures. Both tCBF and pCBF have a strong inverse correlation with the cerebrovascular resistance index, with correlation coefficients of  $r=-0.82$  and  $r=-0.67$ , respectively. Older age, male sex (versus female), and a history of diabetes, hypertension, and coronary heart disease were associated with faster declines in tCBF over time. Older age, female sex, and

a history of hypertension were associated with faster declines in pCBF over time. In contrast, older age, obesity, and a history of hypertension were associated with an increased cerebrovascular resistance index (Table S2).

### Single-Time Point Cerebral Hemodynamics and Progression of Cerebral Small Vessel Disease

As shown in Table 2, lower tCBF, lower pCBF, and higher cerebrovascular resistance index at baseline were all associated with a higher risk of the progression of lacunes, but none were associated with the progression of WMH, microbleeds, or brain atrophy. The risk ratio for developing incident lacunes were 0.81 (95% CI, 0.69–0.95), 0.80 (95% CI, 0.69–0.93), and 1.29 (95% CI, 1.11–1.49) with 1-SD increase in tCBF, pCBF, and cerebrovascular resistance index, respectively.

### Presence of Cerebral Small Vessel Disease and Subsequent Changes in Cerebral Hemodynamics

As shown in Figure 1, lower brain tissue volume and lacune presence at baseline were associated with faster

**Table 1. Participant Characteristics**

Characteristics*	Overall
n	3623
Age at first MRI scan, y	61.4±9.3
Women, %	54.6
Body mass index, kg/m <sup>2</sup>	27.1±4.0
Smoking status, %	
Never	29.5
Past	45.1
Current	25.3
History of cardiovascular disease, %	4.7
History of diabetes, %	8.1
History of hypertension, %	46.6
Systolic blood pressure, mm Hg	132±19
Diastolic blood pressure, mm Hg	80±11
Mean arterial blood pressure, mm Hg	98±13
tCBF, mL·min <sup>-1</sup>	538.1±97.4
pCBF, mL·100·mL <sup>-1</sup> ·min <sup>-1</sup>	56.8±9.3
Cerebrovascular resistance index, mm Hg·mL <sup>-1</sup> ·min <sup>-1</sup>	0.19±0.04
Years between cerebral blood flow measurements	3.6 (1.9–4.1)
Change in tCBF per y, mL·min <sup>-1</sup>	−4.0±36.6
Change in pCBF per y, mL·100·mL <sup>-1</sup> ·min <sup>-1</sup>	−0.3±4.1
Change in cerebrovascular resistance index, mm Hg·mL <sup>-1</sup> ·min <sup>-1</sup>	0.006±0.04

Data are shown in the format of mean±SD, percentage, or median (25th–75th percentiles). MRI indicates magnetic resonance imaging; pCBF, parenchymal cerebral blood flow; and tCBF, total cerebral blood flow.

\*Characteristics at baseline measurement unless otherwise specified.

**Table 2. Single-Time Point Cerebral Hemodynamic Measures and Risk of the Progression of Subclinical Brain Vascular Disease**

	Risk ratio (95% CI) by the quartile of cerebral hemodynamic measure				Risk ratio (95% CI)	P value
	First quartile	Second quartile	Third quartile	Fourth quartile	Per SD increase	
tCBF, mL/min	<469	469–530	530–598	≥598		
White matter hyperintensities	1 (ref)	1.06 (0.94–1.19)	1.10 (0.97–1.24)	1.11 (0.96–1.28)	1.03 (0.97–1.08)	0.338
Cerebral microbleeds	1 (ref)	1.01 (0.81–1.25)	1.04 (0.84–1.30)	0.98 (0.77–1.25)	1.03 (0.95–1.12)	0.453
Lacunae	1 (ref)	0.68 (0.49–0.94)	0.46 (0.32–0.67)	0.71 (0.49–1.03)	0.81 (0.69–0.95)	0.008
Brain atrophy	1 (ref)	1.02 (0.90–1.16)	1.02 (0.89–1.16)	1.00 (0.86–1.16)	0.99 (0.94–1.05)	0.744
pCBF, mL·100 mL <sup>-1</sup> ·min <sup>-1</sup>	<51	51–56	56–62	≥62		
White matter hyperintensities	1 (ref)	1.08 (0.97–1.21)	0.99 (0.87–1.11)	1.08 (0.96–1.23)	1.01 (0.97–1.06)	0.536
Cerebral microbleeds	1 (ref)	1.12 (0.90–1.38)	1.19 (0.96–1.47)	1.00 (0.79–1.26)	1.02 (0.94–1.10)	0.676
Lacunae	1 (ref)	0.70 (0.51–0.98)	0.65 (0.46–0.91)	0.58 (0.40–0.84)	0.80 (0.69–0.93)	0.004
Brain atrophy	1 (ref)	0.97 (0.85–1.10)	0.93 (0.82–1.06)	1.01 (0.89–1.15)	0.99 (0.94–1.04)	0.624
Total cerebrovascular resistance index, mm Hg·mL <sup>-1</sup> ·min <sup>-1</sup>	<0.16	0.16–0.19	0.19–0.22	≥0.22		
White matter hyperintensities	1 (ref)	1.08 (0.94–1.25)	1.07 (0.92–1.24)	0.98 (0.82–1.16)	0.97 (0.92–1.03)	0.306
Cerebral microbleeds	1 (ref)	0.92 (0.73–1.17)	0.89 (0.70–1.14)	0.90 (0.68–1.19)	0.98 (0.89–1.08)	0.667
Lacunae	1 (ref)	1.20 (0.80–1.82)	1.50 (0.99–2.27)	2.01 (1.25–3.22)	1.29 (1.11–1.49)	0.001
Brain atrophy	1 (ref)	0.98 (0.86–1.13)	1.10 (0.95–1.27)	1.07 (0.90–1.26)	1.04 (0.98–1.11)	0.213

tCBF (mL/min) was determined by adding flow rates for the carotid arteries and the basilar artery and expressed in mL/min. pCBF (mL·min<sup>-1</sup>·100 mL<sup>-1</sup>) was derived by dividing tCBF by total brain tissue volume measured at the same time (per 100 mL, defined as the sum of the volume of gray matter and white matter). MRI indicates magnetic resonance imaging; pCBF, parenchymal cerebral blood flow; Ref, reference; and tCBF, total cerebral blood flow.

\*With adjustment for age, sex, smoking habits, body mass index, systolic blood pressure, total cholesterol level, history of diabetes and cardiovascular disease, baseline level of the individual MRI marker, and total brain tissue volume (for tCBF and total cerebrovascular resistance index as the exposures).

tCBF decline, whereas total WMH volume and cerebral microbleed presence were not. Each SD decrease in total brain tissue volume at baseline was associated with a larger annual decline of 1.8 mL·min<sup>-1</sup> ([95% CI, 0.8–2.9] *P*<0.001), and the presence of lacunae was associated with a larger annual decline of 3.3 mL·min<sup>-1</sup> in tCBF ([95% CI, 0.05–6.7] *P*=0.05). Lower brain volume and lacunae were similarly associated with an increase in cerebrovascular resistance index, whereas only higher baseline WMH volume was associated with faster pCBF decline over time.

### Simultaneous Changes in Cerebral Hemodynamics and Subclinical Brain Vascular Disease

As shown in Table 3 and Figure 2, for WMH, both large decreases and increases in tCBF and pCBF were associated with concurrent progression in WMH, exhibiting U-shaped associations. In contrast, an increase in the cerebrovascular resistance index over time was associated with faster progression of WMH, demonstrating a clear dose-response relationship. For microbleeds,

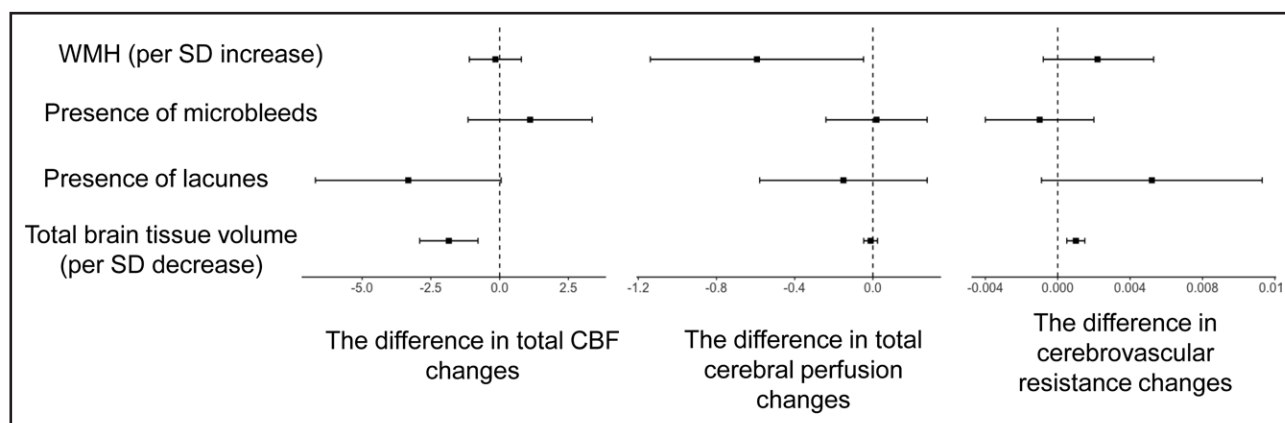


**Figure 1. Subclinical brain disease at baseline and subsequent changes in cerebral hemodynamics.**

Association estimates were adjusted for age, sex, body mass index, systolic blood pressure, total cholesterol level, smoking habits, history of diabetes and coronary heart disease, cerebral hemodynamic measurement, and total brain tissue volume at the initial magnetic resonance imaging scan. pCBF indicates parenchymal cerebral blood flow; tCBF, total cerebral blood flow; and WMH, white matter hyperintensities.

**Table 3. Changes in Cerebral Blood Flow Measures and Risk of the Progression of Subclinical Brain Vascular Disease**

	Cerebral hemodynamic measures (in quartiles)				Risk ratio (95% CI)*	P values‡
	Large decrease (first quartile)	Modest decrease (second quartile)	Stable to modest increase (third quartile)	Large increase (fourth quartile)	Per SD increase†	
Changes in tCBF, mL/min	<-22	-22 to -4	-4 to 15	≥15		
White matter hyperintensities						
No. of events/observations	344/1365	350/1361	347/1364	322/1360		
Risk ratio (95% CI)*	1.36 (1.19 to 1.55)	1.02 (0.91 to 1.14)	1 (ref)	1.28 (1.14 to 1.45)	...	<0.001
Cerebral microbleeds						
No. of events/observations	147/1436	140/1435	148/1435	149/1436		
Risk ratio (95% CI)*	1.24 (0.98 to 1.57)	0.91 (0.74 to 1.13)	1 (ref)	1.26 (1.02 to 1.56)	...	<0.001
Lacunes						
No. of events/observations	54/1436	70/1435	72/1435	60/1436		
Risk ratio (95% CI)*	1.21 (0.84 to 1.76)	1.04 (0.75 to 1.43)	1 (ref)	0.94 (0.67 to 1.32)	0.94 (0.75 to 1.17)	0.574
Brain atrophy						
No. of events/observations	417/1366	309/1361	303/1364	334/1361		
Risk ratio (95% CI)*	1.87 (1.63 to 2.14)	1.07 (0.93 to 1.22)	1 (ref)	1.34 (1.17 to 1.54)	...	<0.001
Changes in pCBF, mL·100-mL <sup>-1</sup> ·min <sup>-1</sup>	<-2	-2 to -0.3	-0.3 to 1.7	≥1.7		
White matter hyperintensities						
No. of events/observations	348/1363	343/1362	350/1368	322/1357		
Risk ratio (95% CI)*	1.39 (1.23 to 1.59)	1.01 (0.89 to 1.13)	1 (ref)	1.24 (1.10 to 1.40)	...	<0.001
Cerebral microbleeds						
No. of events/observations	141/1374	132/1374	144/1374	140/1374		
Risk ratio (95% CI)*	1.25 (0.98 to 1.59)	0.91 (0.73 to 1.13)	1 (ref)	1.21 (0.97 to 1.50)	...	0.001
Lacunes						
No. of events/observations	49/1374	63/1374	64/1374	56/1374		
Risk ratio (95% CI)*	1.27 (0.87 to 1.88)	1.08 (0.77 to 1.53)	1 (ref)	0.96 (0.67 to 1.37)	0.92 (0.73 to 1.14)	0.431
Brain atrophy						
No. of events/observations	368/1363	304/1362	298/1368	393/1359		
Risk ratio (95% CI)*	1.60 (1.38 to 1.84)	1.05 (0.92 to 1.20)	1 (ref)	1.58 (1.39 to 1.80)	...	<0.001
Changes in cerebrovascular resistance index, mm Hg·mL <sup>-1</sup> ·min <sup>-1</sup>	<-0.02	-0.02 to 0.01	0.01 to 0.03	≥0.03		
White matter hyperintensities						
No. of events/observations	301/1254	293/1295	312/1282	358/1271		
Risk ratio (95% CI)*	1 (ref)	1.13 (1.00 to 1.30)	1.25 (1.09 to 1.43)	1.33 (1.16 to 1.52)	1.10 (1.06 to 1.15)	<0.001
Cerebral microbleeds						
No. of events/observations	167/1343	123/1344	128/1344	128/1343		
Risk ratio (95% CI)*	1 (ref)	0.75 (0.60 to 0.94)	0.77 (0.61 to 0.97)	0.72 (0.57 to 0.91)	0.91 (0.83 to 0.99)	0.032
Lacunes						
No. of events/observations	60/1343	50/1344	65/1344	57/1343		
Risk ratio (95% CI)*	1 (ref)	1.22 (0.82 to 1.81)	1.61 (1.10 to 2.36)	1.32 (0.87 to 1.98)	1.05 (0.92 to 1.19)	0.456
Brain atrophy						
No. of events/observations	331/1255	300/1295	315/1282	336/1272		
Risk ratio (95% CI)*	1 (ref)	0.91 (0.79 to 1.05)	0.98 (0.86 to 1.13)	0.99 (0.86 to 1.13)	1.01 (0.96 to 1.06)	0.686

MRI indicates magnetic resonance imaging; pCBF, parenchymal cerebral blood flow; Ref, reference; and tCBF, total cerebral blood flow

\*With adjustment for age, sex, smoking habits, body mass index, systolic blood pressure (for changes in tCBF and pCBF as the exposures), total cholesterol level, history of diabetes and cardiovascular disease, the baseline level of the individual MRI marker, and total brain tissue volume (for changes in tCBF and cerebrovascular resistance index as the exposures).

†Not presented for estimates that appeared to be nonlinear and U-shaped association.

‡P for nonlinearity in the presence of U-shaped association.

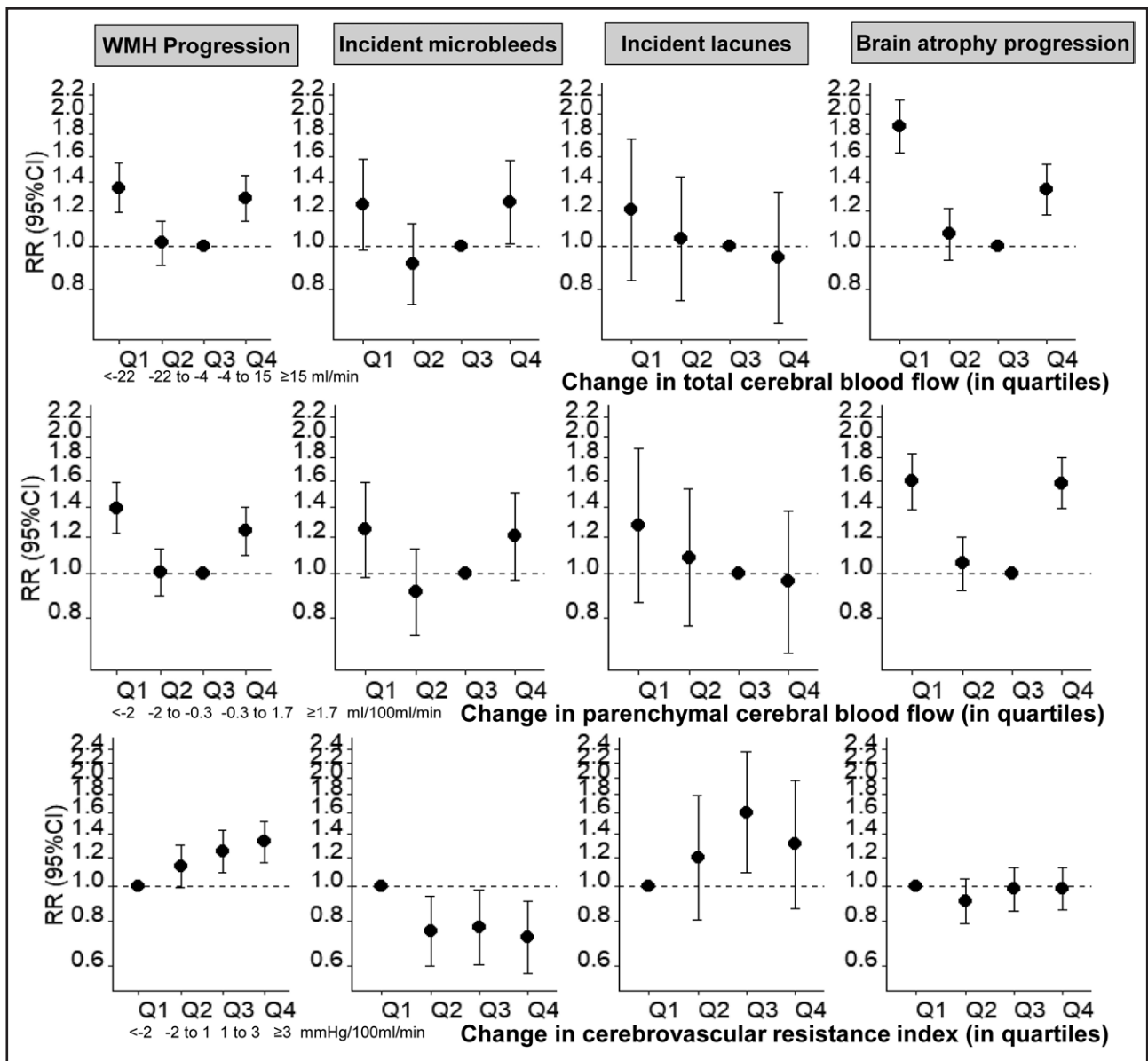


**Figure 2. Longitudinal changes in cerebral hemodynamics and progression of subclinical brain disease.**

Figure shows the risk of progression of brain magnetic resonance imaging (MRI) markers of subclinical brain disease in relation to changes in total cerebral blood flow (top), parenchymal cerebral blood flow (middle), and cerebrovascular resistance index (bottom), after adjustment for age, sex, smoking habits, body mass index, blood pressure level, total cholesterol level, history of diabetes and cardiovascular disease, total cerebral blood flow measures, total brain tissue volume (for total cerebral blood flow and total cerebrovascular resistance index as the exposures) at baseline, and baseline level of individual MRI markers. RR indicates risk ratio; and WMH, white matter hyperintensities.

both large increases and decreases in tCBF and pCBF were similarly associated with a higher risk of incident microbleeds (ie, a U-shaped association). In contrast, an increase in the cerebrovascular resistance index was associated with a lower risk of incident microbleeds in a dose-response manner. For lacunes, although both decreases in tCBF and pCBF and increases in cerebrovascular resistance seem to be associated with increased risk of incident lacunes, none of these associations were statistically significant. For brain atrophy, a U-shaped association with the progression of brain atrophy was observed for changes in tCBF and pCBF, whereas no

association was observed for the cerebrovascular resistance index. Overall, the association patterns with the progression of subclinical brain vascular disease demonstrate clearer associations when cerebral hemodynamics were assessed by cerebrovascular resistance compared with tCBF or pCBF.

### Other Secondary and Sensitivity Analyses

The association estimates with the progression in subclinical brain vascular disease did not essentially change after replacing systolic BP with diastolic BP

and antihypertensive medication use in separate models. The association estimates for the changes in tCBF and pCBF were also similar with additional adjustments for longitudinal changes in systolic BP (Table S3). When stratified by hypertension status, the risk of progression in subclinical brain vascular disease associated with the change in CBF measures was either U-shaped or J-shaped essentially in all subgroups, but the relative risk associated with large decreases and large increases in CBF measures appeared to differ by hypertension status and also vary with individual MRI markers, showing an overall more pronounced U-shaped association in participants without hypertension. In contrast, the associations with the change in cerebrovascular resistance were similar in those with and without hypertension (Table S4). Results were also similar after further adjusting for hemoglobin level (Table S5) and applying inverse probability weights in the models (Table S6). The associations with the change in cerebrovascular resistance index showed the same direction for incident microbleeds in the lobar versus deep regions (Table S7).

## DISCUSSION

In community-dwelling older adults, we found that lower CBF and a higher cerebrovascular resistance index at baseline were associated with incident lacunes but not with the progression of WMH. The presence of subclinical brain vascular disease at baseline was also associated with a subsequent faster decline in CBF and an increase in cerebrovascular resistance over time. Longitudinally, both large decreases and increases in CBF over time were associated with the progression of WMH, brain atrophy, and incident microbleeds, with varying associations by hypertension status. Increases in cerebrovascular resistance index over time were dose-dependently associated with faster progression of WMH but a lower risk of incident microbleeds, regardless of hypertension status. Our findings suggest a bidirectional longitudinal relationship between cerebral hemodynamics and the progression of brain vascular pathology, extending beyond single-time point brain MRI measurements. Changes in CBF and cerebrovascular resistance index may capture distinct pathophysiological mechanisms linking cerebral hemodynamics to subclinical brain disease, with more consistent association patterns observed for cerebrovascular resistance index.

In our study, over half of the participants had declining CBF over 4 years, consistent with previous reports.<sup>18,34</sup> The average decline in CBF is comparable to findings from a previous cross-sectional study among healthy adults, indicating an overall decline associated with physiological brain aging.<sup>35</sup> We observed a U-shaped association between changes in CBF and the progression of WMH, microbleeds, and brain atrophy, as well as an inverse association with incident lacunes that was not statistically significant. This finding suggests that the

pathophysiology of lacunes may differ from other vascular brain lesions, possibly because of greater susceptibility to cerebral hypoperfusion, whereas other lesions may be more prone to unstable CBF over time.<sup>36</sup> Alternatively, it may also reflect hypoperfusion in disconnected areas because of lacune or other ischemic lesions (ie, reverse causation).<sup>37</sup> We observed an association of both large increases and decreases in CBF with the progression of brain vascular markers, especially in those without hypertension. An accelerated decline in CBF may indicate underlying pathophysiological changes associated with cerebral small vessel disease. In contrast, an increase in CBF may reflect the fluctuation of CBF over time, or an intermediate compensatory stage to maintain sufficient oxygen supply and promote the clearance of toxic substances preceding decompensation and cerebral hypoperfusion.<sup>33</sup> This explanation aligns with previous studies reporting that in cognitively normal participants, CBF was higher in high-risk individuals, including those with *APOE e4* allele<sup>23</sup> and cerebral amyloid deposition.<sup>38</sup>

Cerebrovascular resistance index and its longitudinal change were observed to be associated with a higher risk of ischemic-prone lesions and a lower risk of hemorrhagic-prone lesions in a dose-response manner regardless of hypertension status, demonstrating more consistent association patterns compared with CBF. This observation is in concert with previous observations indicating a stronger association of cerebrovascular resistance with Alzheimer pathology and neurodegeneration than CBF alone,<sup>22,23,39</sup> as well as studies linking increased internal carotid artery resistivity to WMH.<sup>40</sup> An increase in cerebrovascular resistance reflects vasoconstriction that narrows blood vessel diameter and may result from increased arterial stiffness and inflammation-induced endothelial dysfunction.<sup>41</sup> Vasoconstriction has been associated with impairment in brain amyloid clearance,<sup>42</sup> whereas the use of vasodilators has been suggested as a potential therapeutic target for facilitating amyloid clearance.<sup>43</sup> These data suggest that cerebrovascular resistance could be a susceptibility marker for brain ischemia.

Our results support the bidirectional relationship between cerebral hemodynamics and subclinical brain vascular disease. On the one hand, fluctuating CBF may increase shear stress toward vessel walls, especially vascular endothelium, contributing to endothelial and microvascular dysfunction.<sup>44</sup> Large decreases in CBF may also lead to cerebral hypoperfusion, contributing to brain ischemia such as lacune and WMH.<sup>45</sup> On the other hand, CBF may decline over time as a result of the reduction in cerebral metabolism demand associated with ischemia and atrophy or increased cerebral vascular resistance.<sup>11,20,46,47</sup> Impaired neurovascular function resulting from cerebrovascular disease and neurodegeneration may also affect CBF.<sup>48</sup> Our observation that a history of hypertension, diabetes, obesity, and coronary heart disease was associated with exaggerated changes

in these cerebral hemodynamic measures underscores the importance of primordial prevention of cardiovascular disease in maintaining normal cerebral hemodynamics and brain health.

Several limitations of our study need to be noted. First, the use of 2-dimensional phase-contrast flow measurement limited our ability to assess region-specific changes in CBF and the underlying pathologies. Second, we assessed the association of the change in CBF with concurrent instead of subsequent progression in subclinical disease. Although our finding sheds light on the underlying vascular pathology associated with longitudinal changes in CBF, it limits our ability to inform the temporal relationship. Third, cerebral microbleeds were assessed using a 3-dimensional T2\*-weighted sequence, which may be less sensitive than the susceptibility-weighted imaging sequence in detecting microbleeds. This may result in nondifferential classification bias and conservative association estimates. Moreover, the assessment of BP and cerebral hemodynamics at resting position during the research visits are also subject to random measurement error and may not adequately capture the real-time highly variable physiological signals, thus potentially leading to regression dilution bias and conservative association estimates. As an observational study, confounding by other factors affecting BP and cerebral hemodynamics, such as changes in lifestyle and medication use, is possible. In addition, we were also unable to effectively assess the impact of different medications on vasodilatation and the observed relationship. Last, as our study focused on the longitudinal changes in neuroimaging assessment, only participants who completed 2 MRI scans were included, which could have introduced selection bias. Our findings should be viewed as exploratory and need to be confirmed in future studies that include region-specific CBF assessment and repeated brain MRI assessment in diverse older populations.

## CONCLUSIONS

Longitudinal changes in CBF and cerebrovascular resistance index may have a bidirectional relationship with the development of subclinical vascular brain disease in older adults in addition to single-time point measurements. The cerebrovascular resistance index might serve as a more sensitive marker than CBF for detecting associations with subclinical cerebrovascular pathology. These results offer novel insights into the pathophysiological mechanisms linking cerebral hemodynamics to subclinical brain disease, and consequently, stroke and dementia.

## ARTICLE INFORMATION

Received April 23, 2024; final revision received October 1, 2024; accepted October 25, 2024.

## Affiliations

Department of Epidemiology, Harvard T.H. Chan School of Public Health, Boston, MA (Y.M., A.H.). Department of Epidemiology (D.B., F.J.W., A.H., M.A.I., M.W.V.), Department of Radiology and Nuclear Medicine (D.B., F.J.W., W.N., M.W.V.), and Department of Medical Informatics (W.N.), Erasmus MC University Medical Center, Rotterdam, the Netherlands. Department of Imaging Science and Technology, Faculty of Applied Sciences, Delft University of Technology, the Netherlands (W.N.).

## Acknowledgments

The authors gratefully acknowledge the dedication, commitment, and contribution of inhabitants, general practitioners, and pharmacists of the Ommoord district to the Rotterdam Study.

## Sources of Funding

The Rotterdam Study is funded by Erasmus Medical Center and Erasmus University, Rotterdam; Netherlands Organisation for the Health Research and Development (ZonMw); the Research Institute for Diseases in the Elderly (the Ministry of Education, Culture and Science; the Ministry for Health, Welfare, and Sports; the European Commission (DG XII); and the Municipality of Rotterdam. This work was also supported by a grant (R00AG071742, to Dr Ma) from the National Institutes of Health. Dr Wolters receives research funding from the Netherlands Organisation for Health Research and Development (ZonMw; Veni-09150162010108 and BIRD-NL-10510032120005), the Dutch Heart Foundation (CVON2018-28), and the Alzheimer's Association (AARF-22-924982), all paid to the institution. The funding organizations had no role in the design and conduct of the study; collection, management, analysis, and interpretation of the data; preparation, review, or approval of the manuscript; and decision to submit the manuscript for publication.

## Disclosures

Dr Niessen received stock from Quantib, which is not directly related to the present article. The other authors report no conflicts.

## Supplemental Material

STROBE Checklist  
Figure S1  
Tables S1–S7

## REFERENCES

- Cipolla M. *The Cerebral Circulation*. Morgan & Claypool Life Sciences; 2009.
- Lassen NA. Cerebral blood flow and oxygen consumption in man. *Physiol Rev*. 1959;39:183–238. doi: 10.1152/physrev.1959.39.2.183
- Strandgaard S, Olesen J, Skinhoj E, Lassen NA. Autoregulation of brain circulation in severe arterial hypertension. *Br Med J*. 1973;1:507–510. doi: 10.1136/bmj.1.5852.507
- Naritomi H, Meyer JS, Sakai F, Yamaguchi F, Shaw T. Effects of advancing age on regional cerebral blood flow. *Arch Neurol*. 1979;36:410–416. doi: 10.1001/archneur.1979.00500430040005
- Glodzki L, Rusinek H, Tsui W, Pirraglia E, Kim HJ, Deshpande A, Li Y, Storey P, Randall C, Chen J, et al. Different relationship between systolic blood pressure and cerebral perfusion in subjects with and without hypertension. *Hypertension*. 2019;73:197–205. doi: 10.1161/HYPERTENSIONAHA.118.11233
- Wolters FJ, De Bruijn RFAG, Hofman A, Koudstaal PJ, Ikram MA. Cerebral vasoreactivity, apolipoprotein E, and the risk of dementia. *Atertio Thromb Vasc Biol*. 2016;36:204–210. doi: 10.1161/atvbaha.115.306768
- Wolters FJ, Zonneveld HI, Hofman A, van der Lugt A, Koudstaal PJ, Vernooij MW, Ikram MA. Cerebral perfusion and the risk of dementia: a population-based study. *Circulation*. 2017;136:719–728. doi: 10.1161/circulationaha.117.027448
- Jordan JD, Powers WJ. Cerebral autoregulation and acute ischemic stroke. *Am J Hypertens*. 2012;25:946–950. doi: 10.1038/ajh.2012.53
- Sabayan B, Van Der Grond J, Westendorp RG, Jukema JW, Ford I, Buckley BM, Sattar N, Van Osch MJ, Van Buchem MA, De Craen AJM. Total cerebral blood flow and mortality in old age: a 12-year follow-up study. *Neurology*. 2013;81:1922–1929. doi: 10.1212/01.wnl.0000436618.48402.da
- Fani L, Bos D, Mutlu U, Portegies MLP, Zonneveld HI, Koudstaal PJ, Vernooij MW, Ikram MA, Ikram MK. Global brain perfusion and the risk of transient ischemic attack and ischemic stroke: the Rotterdam Study. *J Am Heart Assoc*. 2019;8:e011565. doi: 10.1161/JAHA.118.011565
- Van Der Veen PH, Muller M, Vincken KL, Hendrikse J, Mali WPTM, Van Der Graaf Y, Geerlings MI. Longitudinal relationship between cerebral small-vessel disease and cerebral blood flow: the second manifestations of

- arterial disease-magnetic resonance study. *Stroke*. 2015;46:1233–1238. doi: 10.1161/strokeaha.114.008030
12. Shi Y, Thrippleton MJ, Makin SD, Marshall I, Geerlings MI, De Craen AJ, Van Buchem MA, Wardlaw JM. Cerebral blood flow in small vessel disease: a systematic review and meta-analysis. *J Cereb Blood Flow Metab*. 2016;36:1653–1667. doi: 10.1177/0271678x16662891
  13. Van Elderen SGC, Brandts A, Van Der Grond J, Westenbergh JJM, Kroft LJM, Van Buchem MA, Smit JWA, De Roos A. Cerebral perfusion and aortic stiffness are independent predictors of white matter brain atrophy in type 1 diabetic patients assessed with magnetic resonance imaging. *Diabetes Care*. 2011;34:459–463. doi: 10.2337/dc10-1446
  14. Appelman AP, Van Der Graaf Y, Vincken KL, Tiehuis AM, Witkamp TD, Mali WP, Geerlings MI. Total cerebral blood flow, white matter lesions and brain atrophy: the SMART-MR study. *J Cereb Blood Flow Metab*. 2008;28:633–639. doi: 10.1038/sjcbfm.9600563
  15. Stewart CR, Stringer MS, Shi Y, Thrippleton MJ, Wardlaw JM. Associations between white matter hyperintensity burden, cerebral blood flow and transit time in small vessel disease: an updated meta-analysis. *Front Neurol*. 2021;12:647848. doi: 10.3389/fneur.2021.647848
  16. Ogoh S, Ainslie PN. Cerebral blood flow during exercise: mechanisms of regulation. *J Appl Physiol (1985)*. 2009;107:1370–1380. doi: 10.1152/jappphysiol.00573.2009
  17. Conroy DA, Spielman AJ, Scott RO. Daily rhythm of cerebral blood flow velocity. *J Circadian Rhythms*. 2005;3:3. doi: 10.1186/1740-3391-3-3
  18. Beason-Held LL, Moghekar A, Zonderman AB, Kraut MA, Resnick SM. Longitudinal changes in cerebral blood flow in the older hypertensive brain. *Stroke*. 2007;38:1766–1773. doi: 10.1161/STROKEAHA.106.477109
  19. Thambisetty M, Beason-Held L, An Y, Kraut MA, Resnick SM. APOE  $\epsilon$ 4 genotype and longitudinal changes in cerebral blood flow in normal aging. *Arch Neurol*. 2010;67:93–98. doi: 10.1001/archneurol.2009.913
  20. Zonneveld HI, Loehrer EA, Hofman A, Niessen WJ, Lugt AVD, Krestin GP, Ikram MA, Vernooij MW. The bidirectional association between reduced cerebral blood flow and brain atrophy in the general population. *J Cereb Blood Flow Metab*. 2015;35:1882–1887. doi: 10.1038/jcbfm.2015.157
  21. Skow RJ, Brothers RM, Claassen JAHR, Day TA, Rickards CA, Smirl JD, Brassard P. On the use and misuse of cerebral hemodynamics terminology using transcranial Doppler ultrasound: a call for standardization. *Am J Physiol Heart Circ Physiol*. 2022;323:H350–H357. doi: 10.1152/ajpheart.00107.2022
  22. Yew B, Nation DA; Alzheimer's Disease Neuroimaging Initiative. Cerebrovascular resistance: effects on cognitive decline, cortical atrophy, and progression to dementia. *Brain*. 2017;140:1987–2001. doi: 10.1093/brain/aww112
  23. Dounavi ME, Low A, McKiernan EF, Mak E, Muniz-Terrera G, Ritchie K, Ritchie CW, Su L, O'Brien JT. Evidence of cerebral hemodynamic dysregulation in middle-aged APOE  $\epsilon$ 4 carriers: the PREVENT-Dementia study. *J Cereb Blood Flow Metab*. 2021;41:2844–2855. doi: 10.1177/0271678x211020863
  24. Ikram MA, Brusselle GGO, Murad SD, van Duijn CM, Franco OH, Goedegebure A, Klaver CCW, Nijsten TEC, Peeters RP, Stricker BH, et al. The Rotterdam Study: 2018 update on objectives, design and main results. *Eur J Epidemiol*. 2017;32:807–850. doi: 10.1007/s10654-017-0321-4
  25. Ikram MA, van der Lugt A, Niessen WJ, Koudstaal PJ, Krestin GP, Hofman A, Bos D, Vernooij MW. The Rotterdam Scan Study: design update 2016 and main findings. *Eur J Epidemiol*. 2015;30:1299–1315. doi: 10.1007/s10654-015-0105-7
  26. Vernooij MW, van der Lugt A, Ikram MA, Wielopolski PA, Vrooman HA, Hofman A, Krestin GP, Breteler MM. Total cerebral blood flow and total brain perfusion in the general population: the Rotterdam Scan Study. *J Cereb Blood Flow Metab*. 2008;28:412–419. doi: 10.1038/sjcbfm.9600526
  27. de Boer R, Vrooman HA, van der Lijn F, Vernooij MW, Ikram MA, van der Lugt A, Breteler MM, Niessen WJ. White matter lesion extension to automatic brain tissue segmentation on MRI. *Neuroimage*. 2009;45:1151–1161. doi: 10.1016/j.neuroimage.2009.01.011
  28. Ma Y, Yilmaz P, Bos D, Blacker D, Viswanathan A, Ikram MA, Hofman A, Vernooij MW, Ikram MK. Blood pressure variation and subclinical brain disease. *J Am Coll Cardiol*. 2020;75:2387–2399. doi: 10.1016/j.jacc.2020.03.043
  29. Bos MJ, Koudstaal PJ, Hofman A, Ikram MA. Modifiable etiological factors and the burden of stroke from the Rotterdam study: a population-based cohort study. *PLoS Med*. 2014;11:e1001634. doi: 10.1371/journal.pmed.1001634
  30. Zeger SL, Liang KY. Longitudinal data analysis for discrete and continuous outcomes. *Biometrics*. 1986;42:121–130. doi: 10.1097/EDE.0000000000000620
  31. Durrleman S, Simon R. Flexible regression models with cubic splines. *Stat Med*. 1989;8:551–561. doi: 10.1002/sim.4780080504
  32. Lepage B, Lamy S, Dedieu D, Savy N, Lang T. Estimating the causal effect of an exposure on change from baseline using directed acyclic graphs and path analysis. *Epidemiology*. 2015;26:122–129. doi: 10.1097/EDE.0000000000000192
  33. Wolters FJ, Zonneveld HI, Licher S, Cremers LGM, Heart Brain Connection Collaborative Research Group, Ikram MK, Koudstaal PJ, Vernooij MW, Ikram MA. Hemoglobin and anemia in relation to dementia risk and accompanying changes on brain MRI. *Neurology*. 2019;93:e917–e926. doi: 10.1212/wnl.0000000000008003
  34. Muller M, van der Graaf Y, Visseren FL, Mali WP, Geerlings MI. Hypertension and longitudinal changes in cerebral blood flow: the SMART-MR study. *Ann Neurol*. 2012;71:825–833. doi: 10.1002/ana.23554
  35. Marchal G, Rioux P, Petit-Taboué MC, Sette G, Travère JM, Le Poec C, Courtheoux P, Derlon JM, Baron JC. Regional cerebral oxygen consumption, blood flow, and blood volume in healthy human aging. *Arch Neurol*. 1992;49:1013–1020. doi: 10.1001/archneur.1992.00530340029014
  36. Fanning JP, Wesley AJ, Wong AA, Fraser JF. Emerging spectra of silent brain infarction. *Stroke*. 2014;45:3461–3471. doi: 10.1161/STROKEAHA.114.005919
  37. Feeney DM, Baron JC. Diaschisis. *Stroke*. 1986;17:817–830. doi: 10.1161/01.STR.17.5.817
  38. Schultz A, McLaren D, Chhatwal J, Evans K, Johnson K, Sperling R. IC-P-101: increased cerebral blood flow in cognitively normal older adults with amyloid. *Alzheimer's Dement*. 2013;9:P58–P59. doi: 10.1016/j.jalz.2013.05.098
  39. Beishon L, Haunton VJ, Panerai RB, Robinson TG. Cerebral hemodynamics in mild cognitive impairment: a systematic review. *J Alzheimer's Dis*. 2017;59:369–385. doi: 10.3233/JAD-170181
  40. de la Cruz-Cosme C, Dawid-Milner MS, Ojeda-Burgos G, Gallardo-Tur A, Segura T. Doppler resistivity and cerebral small vessel disease: hemodynamic structural correlation and usefulness for the etiological classification of acute ischemic stroke. *J Stroke Cerebrovasc Dis*. 2018;27:3425–3435. doi: 10.1016/j.jstrokecerebrovasdis.2018.08.001
  41. Ziemann SJ, Melenovsky V, Kass DA. Mechanisms, pathophysiology, and therapy of arterial stiffness. *Arterio Thromb Vasc Biol*. 2005;25:932–943. doi: 10.1161/01.atv.0000160548.78317.29
  42. Shin HK, Jones PB, Garcia-Alloza M, Borrelli L, Greenberg SM, Bacskai BJ, Frosch MP, Hyman BT, Moskowitz MA, Ayata C. Age-dependent cerebrovascular dysfunction in a transgenic mouse model of cerebral amyloid angiopathy. *Brain*. 2007;130:2310–2319. doi: 10.1093/brain/awm156
  43. Maki T, Okamoto Y, Carare RO, Hase Y, Hattori Y, Hawkes CA, Saito S, Yamamoto Y, Terasaki Y, Ishibashi-Ueda H, et al. Phosphodiesterase III inhibitor promotes drainage of cerebrovascular  $\beta$ -amyloid. *Ann Clin Transl Neurol*. 2014;1:519–533. doi: 10.1002/acn3.79
  44. Peterson EC, Wang Z, Britz G. Regulation of cerebral blood flow. *Int J Vasc Med*. 2011;2011:1–8. doi: 10.1155/2011/823525
  45. Goldberg MP, Ransom BR. New light on white matter. *Stroke*. 2003;34:330–332. doi: 10.1161/01.str.0000054048.22626.b9
  46. Villringer A, Dirnagl U. Coupling of brain activity and cerebral blood flow: basis of functional neuroimaging. *Cerebrovasc Brain Metab Rev*. 1995;7:240–276.
  47. Zonneveld H, Loehrer E, Krestin G, Niessen W, Hofman A, Ikram MA, Vernooij M. Longitudinal change in total cerebral blood flow and parenchymal cerebral blood flow in the general aging population. *Alzheimer's Dement*. 2014;10:P700. doi: 10.1016/j.jalz.2014.05.1283
  48. Lok J, Gupta P, Guo S, Kim WJ, Whalen MJ, van Leyen K, Lo EH. Cell-cell signaling in the neurovascular unit. *Neurochem Res*. 2007;32:2032–2045. doi: 10.1007/s11064-007-9342-9